Article, Published Version

Scheres, Babette; Schüttrumpf, Holger

Spatial aspects of wave overtopping for seadikes

Die Küste

Zur Verfügung gestellt in Kooperation mit/Provided in Cooperation with:
Kuratorium für Forschung im Küsteningenieurwesen (KFKI)

Verfügbar unter/Available at: https://hdl.handle.net/20.500.11970/105222

Vorgeschlagene Zitierweise/Suggested citation:
Scheres, Babette; Schüttrumpf, Holger (2013): Spatial aspects of wave overtopping for seadikes. In: Die Küste 80. Karlsruhe: Bundesanstalt für Wasserbau. S. 79-110.

Spatial aspects of wave overtopping for seadikes

Babette Scheres and Holger Schüttrumpf

Summary

Within the HYDRALAB IV project CornerDike wave overtopping processes and the influence of very oblique waves and a corner in the dike line on wave overtopping have been investigated on a 1:4 sloped, convexly curved dike model. The test program covered angles of wave attack up to 112.5° for long crested waves and short crested waves with directional spreadings of $\sigma = 12°$ and $\sigma = 34°$. Results showed that the influence of the corner in the dike line depends for $\beta \leq 45°$ on the angle of wave attack and the wave parameters. Increased overtopping discharges at the corner were observed for high waves (here $H_S = 0.15$ m). Tests with long crested and swell-like ($\sigma = 12°$) waves showed no significant influence of the corner on wave overtopping for angles of wave attack between 45° and 75°. For $\beta > 75°$ the influence of oblique wave attack and a corner in the dike line depends greatly on the point of interest: higher mean overtopping discharges were found along the adjacent straight dike arms than next to the dike corner. This issue may be ascribed to diffraction and refraction effects. For high angles of wave attack increased wave overtopping was observed for short crested waves with $\sigma = 34°$ compared to long crested and swell-like waves due to the directional spread.

Keywords

wave overtopping, mean overtopping discharge, very oblique wave attack, curved dike line, dike corner, wave transformation, physical modelling

Zusammenfassung

Im Rahmen des HYDRALAB IV CornerDike-Projektes wurde der Einfluss von sehr schrägem Wellenangriff und einer Ecke in der Deichlinie auf den Wellenüberlauf an einem 1:4 geneigten, konvex gekrümmten Deichmodell untersucht. Das Testprogramm beinhaltete Wellenangriffswinkel bis zu 112,5° für langkämmige Wellen und kurzkämmige Wellen mit Spreadings von $\sigma = 12°$ und $\sigma = 34°$. Die Auswertungen zeigen, dass der Einfluss der Deichecke für $\beta \leq 45°$ von der Wellenangriffsrichtung und den Wellenparametern abhängt. Erhöhter Wellenüberlauf an der Ecke wurde für hohe Wellen festgestellt (hier $H_S = 0{,}15$ m). Tests mit langkämmigen und schwell-ähnlichen ($\sigma = 12°$) Wellen zeigten für β zwischen 45° und 75° keinen signifikanten Einfluss der Ecke auf den Wellenüberlauf. Für $\beta > 75°$ hängt der Einfluss des schrägen Wellenangriffs und der Deichecke stark von der betrachteten Stelle ab: entlang der benachbarten gerade verlaufenden Deicharme wurden höhere mittlere Wellenüberlaufraten festgestellt als an der Deichecke. Diese Beobachtung könnte auf Diffraktions- und Refraktionseffekte zurückzuführen sein. Für kurzkämmigen Seegang mit $\sigma = 34°$ wurden bei hohen Wellenangriffswinkeln, infolge der stärker gestreuten Wellenrichtungen, höhere Überlaufraten als bei langkämmigem und schwell-ähnlichem Seegang festgestellt.

Schlagwörter

Wellenüberlauf, mittlere Wellenüberlaufrate, sehr schräger Wellenangriff, gekrümmte Deichlinie, Deichecke, Wellentransformation, physikalische Modellversuche

Contents

1 Introduction

Hydraulic-engineering structures, e. g. dikes, can be found along coastlines and rivers all over the world to protect against severe storm surges. Hydraulic processes on these structures, such as wave run-up and wave overtopping, are still investigated to develop and optimize design guidance.

Mathematically exact descriptions for the hydraulic processes during wave run-up and wave overtopping on dikes do not exist due to the stochastic nature of these processes. Thus, empirical formulae, which have been obtained from laboratory experiments, help to design straight-aligned dikes by considering the wave run-up heights and wave overtopping discharges. Several effects, caused by e. g. different roughnesses, geometry variations and oblique wave attack, are already considered in these equations to a certain extent.

As incoming waves seldom approach the dike line perpendicularly and sometimes even move parallel to the structure, knowledge about wave run-up and wave overtopping processes under oblique wave attack is required. Yet, no information is given on the effect of waves that move nearly parallel to the dike or even slightly offshore away from the dike.

Some coastlines do not only include straight-aligned dikes, but also concave (bent inland) or convex (bent to the sea) sections as a result of geological characteristics or anthropogenic influences (see Fig. 1). The effect of a corner in the dike line on wave run-up and wave overtopping processes still has to be investigated.

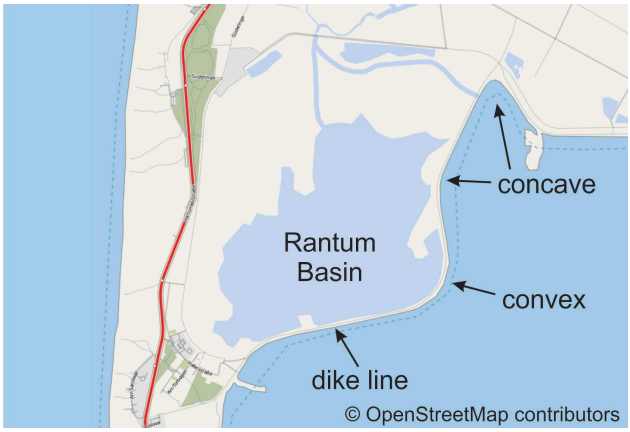

Figure 1: Aerial view of the Rantum Basin on Sylt, Germany [adapted from OPENSTREETMAP].

The main objective of this study is to analyze the influence of very oblique waves and the effect of a corner in the dike line on wave overtopping. The investigations are conducted within the project CornerDike – HyIV-DHI-05. Laboratory tests have been performed on a convex formed dike. A description of the model tests and analysis results on wave overtopping are given in the following.

2 Literature review on wave overtopping

The mean overtopping discharge is a key parameter for designing coastal structures. An overview of methods to assess wave overtopping is given in the EUROTOP-MANUAL (2007).

Approaching waves with run-up heights that exceed the freeboard height (vertical distance between still water level and crest height) lead to wave overtopping. The magnitude of wave overtopping depends on the ratio between the freeboard height and wave run-up height. The EUROTOP-MANUAL (2007) suggests the following formulae for probabilistic calculations, predictions of wave overtopping and comparisons of measurements for coastal dikes:

$$\frac{q}{\sqrt{g \cdot H_{m0}^3}} = \frac{0.067}{\sqrt{\tan\alpha}} \cdot \gamma_b \cdot \xi_{m-1,0} \cdot \exp\left(-4.75 \frac{R_c}{\xi_{m-1,0} \cdot H_{m0} \cdot \gamma_b \cdot \gamma_f \cdot \gamma_\beta \cdot \gamma_v} \right) \quad (1)$$

$$\text{with a maximum of} \quad \frac{q}{\sqrt{g \cdot H_{m0}^3}} = 0.2 \cdot \exp\left(-2.6 \frac{R_c}{H_{m0} \cdot \gamma_f \cdot \gamma_\beta} \right) \quad (2)$$

with:
- g gravity acceleration [m/s²]
- H_{m0} significant wave height [m]
- α angle between dike slope and horizontal [°]
- R_c freeboard height [m]
- $\xi_{m-1,0}$ = $\tan\alpha/(H_{m0}/L_{m-1,0})^{1/2}$ breaker parameter based on spectral period $T_{m-1,0}$ [-]
- γ_b correction factor for a berm [-]
- γ_f correction factor for the permeability and roughness of or on the slope [-]
- γ_β correction factor for oblique wave attack [-]
- γ_v correction factor for a crest wall on the slope [-]

Different surfaces of the seaward slope and dike crest of coastal dikes can be found, each influencing wave overtopping to a certain extent. The effect of the surface roughness is considered in wave overtopping predictions with a correction factor for the permeability and roughness of or on the slope γ_f. Examples and detailed information are given in the EUROTOP-MANUAL (2007). A concrete cover corresponds to a smooth, impermeable surface that is considered with a correction factor of $\gamma_f = 1.0$. The influences of a berm or a crest wall are not explained any further here. Methods to consider the influence of oblique wave attack on wave overtopping are presented in the following.

Oblique waves are described by the angle of wave attack β at the toe of the structure, which is defined as the angle between the direction of approaching waves and the normal line to the dike axis (see Fig. 2). $\beta = 0°$ is equivalent to waves that approach perpendicularly to the dike.

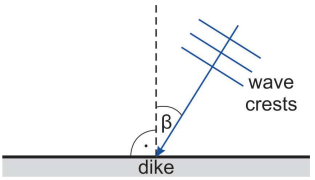

Figure 2: Definition of the angle of wave attack β (adapted from EUROTOP-MANUAL 2007).

The influence of oblique wave attack on wave overtopping is considered with the correction factor γ_β. Results of investigations on the influence of oblique waves show that wave overtopping discharges decrease with increasing angle of wave attack β (see DE WAAL and VAN DER MEER 1992; KORTENHAUS et al. 2006; LORKE et al. 2010). Some investigations found no influence for small angles of wave attack $\beta < 20°$ (cf. OUMERACI et al. 2001; NAPP et al. 2004). Only little knowledge exists for $\beta > 60°$. No validated guidance is given for $\beta > 80°$. Wave overtopping is assumed to be $q = 0$ for angles of wave attack $\beta > 110°$. Recommended formulae of γ_β for sloped structures are plotted against the angle of wave attack β in Fig. 3.

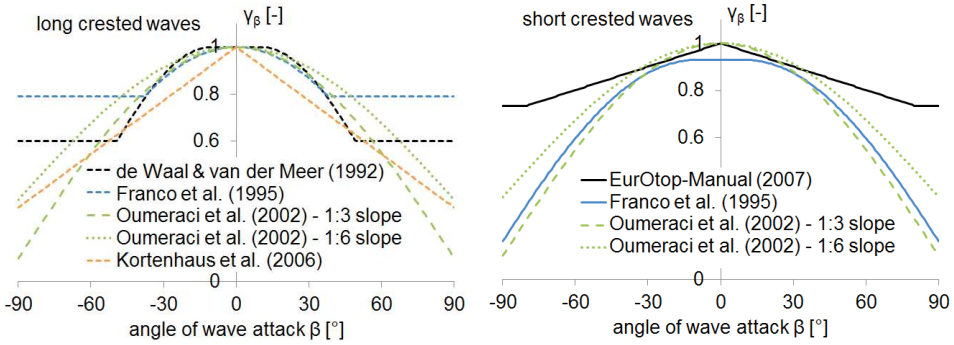

Figure 3: Correction factor γ_β from previous investigations for long crested waves (left) and short crested waves (right) plotted against angle of wave attack β.

Multidirectional waves lead for perpendicular wave attack to slightly lower overtopping discharges than unidirectional waves. The difference may lie in the range of scattering (see OUMERACI et al. 2001). Considering the angle of wave attack β, differences in the behavior of wave overtopping during tests with long crested and short crested waves have been observed. These are partly considered by giving recommendations depending on the wave crestedness (cf. Fig. 3).

High wave overtopping was observed at re-entrant corners during field observations. SAKAKIYAMA and KAJIMA (1996) and NAPP et al. (2002) carried out laboratory experiments on models of seawalls with convex or concave corners. Results of these investigations cannot be applied to sloped structures. Hence, no clear statement on the effects of a corner in the dike line can be given yet.

Overall, investigations are required to analyze the influence of very oblique and slightly offshore ($\beta > 90°$) waves and a corner in the dike line. Therefore, the CornerDike project was originated to develop and enhance the design guidance for seadikes.

3 CornerDike project

3.1 Experimental set-up

The model tests were performed in the shallow water basin of the Danish Hydraulic Institute (DHI) in Hørsholm, Denmark. This 35 m long and 25 m wide basin with an overall depth of 0.8 m can be used for combined wave and current tests. A multidirectional segmented wave maker was installed along the east side of the basin.

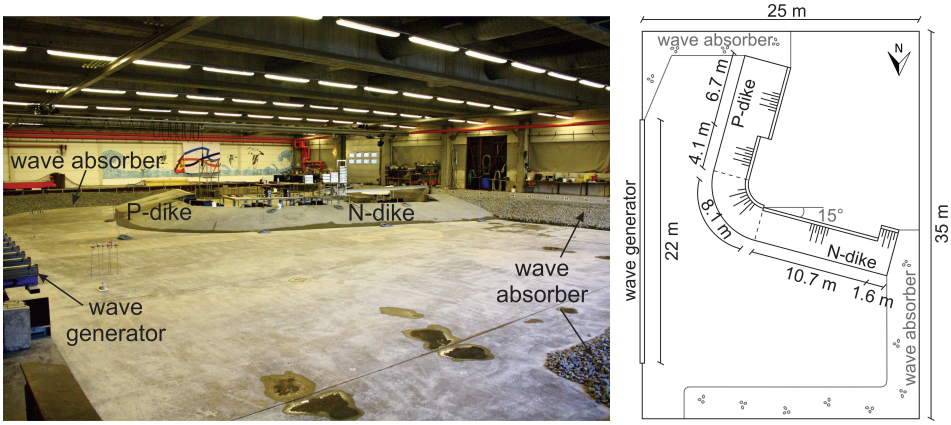

Figure 4: Overview of the model set-up (left) and plan view (right).

The investigated dike was built up in the southern part of the basin. The model set-up is given in Fig. 4. For the CornerDike project, the 18 m long wave maker had to be extended on the southern side by a 4 m long portable wave maker (see Fig. 5). The 44 segments of this combined wave generator had a width of 0.5 m and a height of 1.2 m each and could be used to generate 2D and 3D waves with a maximum wave height of 0.55 m at a period of 2.3 s.

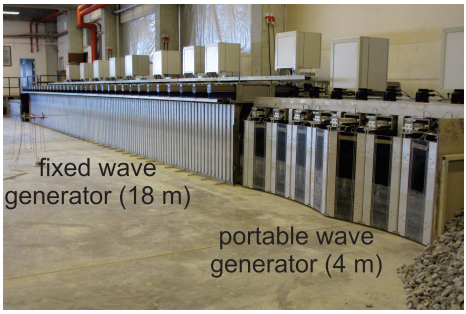

Figure 5: Fixed and portable wave generator.

Stone rip-rap was used as wave absorber to reduce wave reflection and diffraction to a minimum. Therefore, heaps of gravel were placed along the vertical borders of the basin (cf. Fig. 4).

The model tests were performed for a 1:4 sloped dike, which is typical for river and coastal dikes. The dike is convex formed with an angle of 90° and thus can be divided into two sections: The P-dike, which is almost parallel to the wave generator, and the N-dike, which is rectangular (normal) to the P-dike. The whole dike construction is rotated by 15° to provide a fully developed wave field at the N-dike and to ensure that those angles of wave attack that were neglected in the past can be investigated during the CornerDike project. The crest heights were adjusted to 0.75 m at the P-dike and 0.7 m at the N-dike. Parts of the dike that were not required during the overtopping tests had a crest height of 1.0 m as a preparation for run-up tests, for which the dike height had to be increased.

3.2 Measuring instrumentation

An overview of all measuring devices that were used during the overtopping tests is given in Fig. 6. The blue marked area illustrates the range of investigated wave directions.

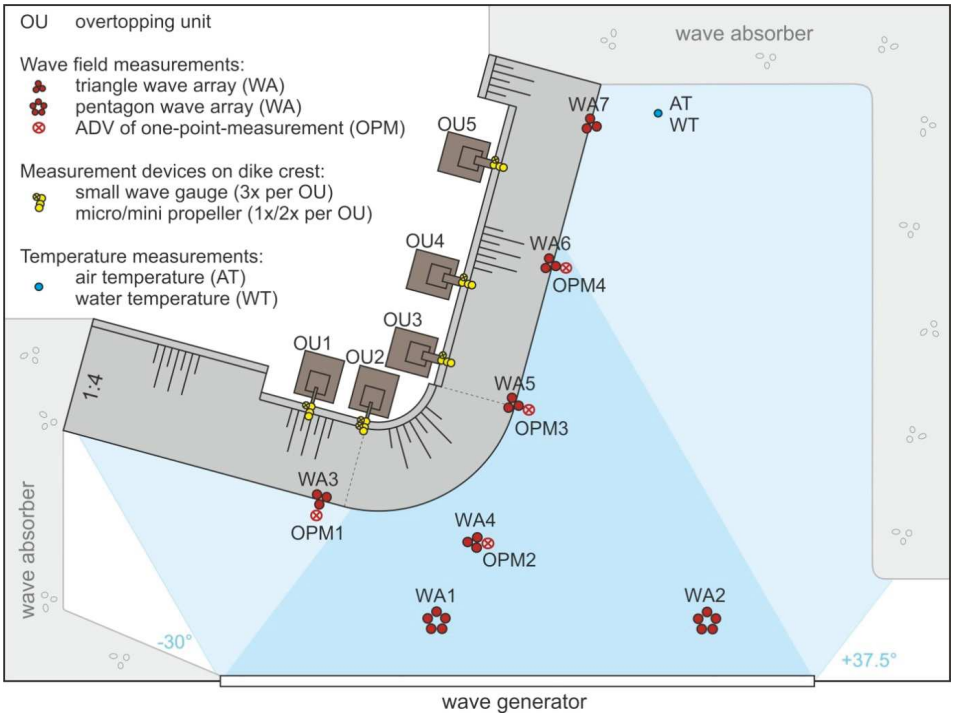

Figure 6: Overview of all measuring devices for the overtopping tests.

3.2.1 Wave field – wave arrays and one-point-measurements

The wave field was measured at seven positions (see Fig. 6). To consider the wave crestedness, the following configurations of wave field measurements were chosen:

- Wave arrays WA (three wave gauges in triangle-configuration or five wave gauges in pentagon-configuration)
- One-point-measurements OPM (one wave gauge and one ADV)

Two wave arrays in pentagon-configuration were installed in front of the wave generator (see WA1 and WA2 in Fig. 6). Moreover three one-point-measurements were placed at the toe of the dike (OPM1, OPM3 and OPM4). OPM2 was fixed at the intersection point of the extension lines of both dike arms to observe the development of the wave field. Each of these four one-point-measurements was extended by two further wave gauges to create another opportunity for wave field analysis (three wave gauges in a triangle-configuration, WA3 to WA6). Additionally, a wave array in triangle-configuration (WA7) was attached at the toe of the N-dike near overtopping unit no. 5.

The one-point-measurements consisted each of one wave gauge and one ADV (Acoustic Doppler Velocimeter), which were installed close to each other. Fig. 7 shows one of the one-point-measurements.

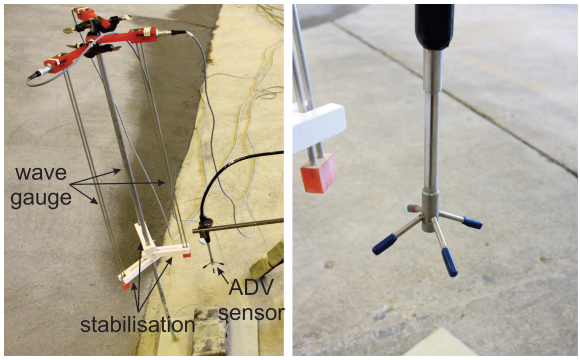

Figure 7: One-point-measurement (left) and close-up of ADV sensor (right).

The wave arrays were built up of three large wave gauges positioned in a triangle or of five large wave gauges installed in a pentagon. Fig. 8 illustrates the triangle- and the pentagon-configuration.

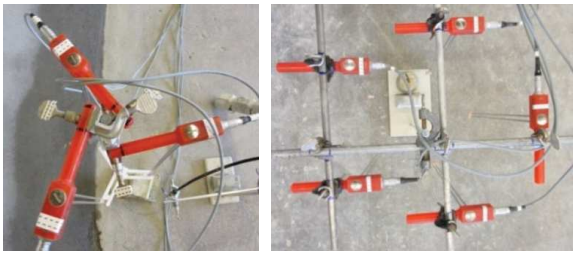

Figure 8: Triangle-configuration (left) and pentagon-configuration (right).

Time domain and frequency domain wave field analyses were performed with DHI MIKE Zero and the WAFO-tool (Wave Analysis for Fatigue and Oceanography). No reflection analysis could be performed with DHI MIKE Zero or the WAFO-tool. Hence, only the measured wave parameters (not the wave parameters of the incident waves!) could be determined with these software programs. The use of the measured wave parameters is considered to be appropriate due to the low reflection of the smooth structure.

3.2.2 Overtopping volume – weighing cells and pumps

Three overtopping units were built up behind the N-dike and two behind the P-dike to measure the amount of overtopped water. All overtopping units were made of plywood and were constructed identically except for different inlet channel widths at the P-dike and N-dike (see below). Fig. 9 illustrates the overtopping units and gives the exact positions.

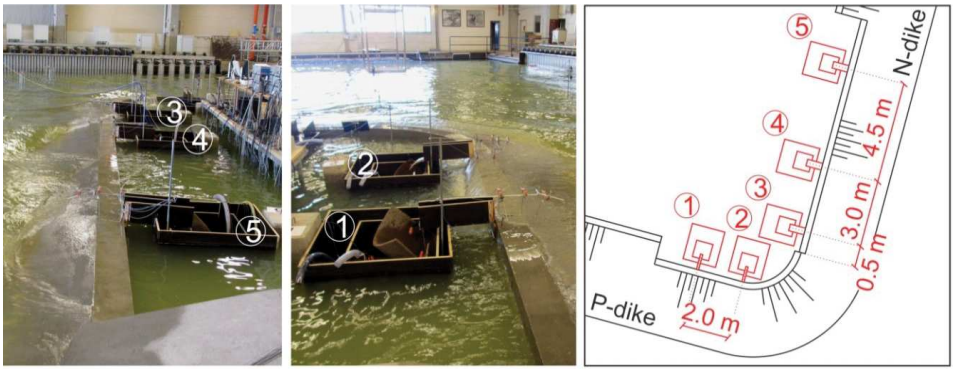

Figure 9: Overtopping units at N-dike (left) and at P-dike (middle), set-up of overtopping units (right).

Fig. 10 shows a cross section of an overtopping unit at the P-dike. Overtopping water flows over an overflow channel into the inner tank (0.75 m x 0.75 m x 0.43 m). In this inner tank the weight of overtopping water is measured by a 0.1 m high weighing cell, which was fixed beneath the inner tank. The outer box contained the weighing cell and the inner tank. This way the weighing cell and inner tank were positioned in a dry area and prevented from uplifting. The wall of the outer box next to the dike was extended to avoid water splashing into the inner tank. Additionally, a mat was placed in the overtopping tank to reduce the noise of the signals, which occurred due to the inflow of water and impact on the bottom of the inner tank. Standard pumps installed in the inner tanks were used to empty the inner tanks during and after the tests. Furthermore, pumps were used in the outer boxes to keep the water level in these boxes as low as possible in the case that there was a leak.

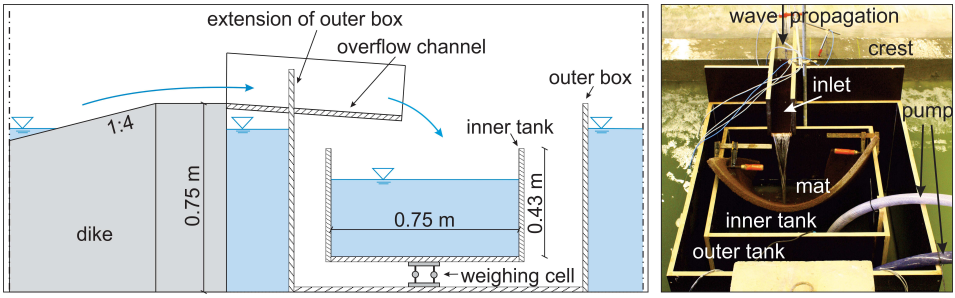

Figure 10: Cross-section of overtopping unit at P-dike (left) and overtopping unit at P-dike seen from behind the dike (right).

As the predicted mean overtopping discharges were higher for the P-dike than for the N-dike, the width of the inlet channels was chosen 0.1 m at the P-dike and 0.3 m at the N-dike to adjust the overtopping volumes. The gap between overtopping channel and dike crest was filled up with silicone to smoothen the junction and to prevent any water intrusion.

3.2.3 Measurements on the dike crest – mini/micro propellers and small wave gauges

Flow processes can be investigated using the signals of 15 small wave gauges, two mini propellers and four micro propellers (manufactured by the Swiss company Schiltknecht). These devices were installed on the dike crest and on the slope (see Fig. 11).

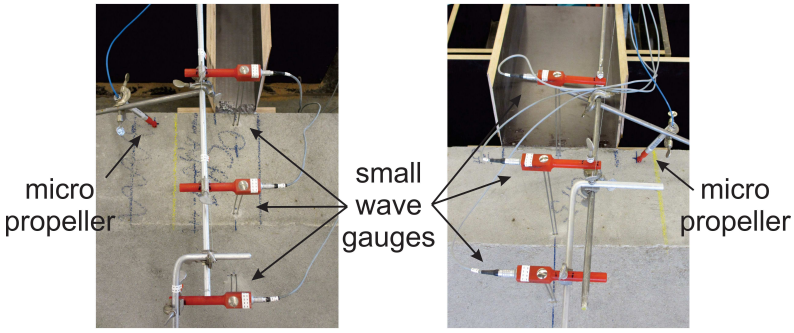

Figure 11: Configuration of instrumentation on the dike crest of P-dike (left) and N-dike (right).

3.3 Test program

The test program covered tests with wave directions α from -30° to +37.5° with respect to the wave generator. Fig. 12 gives the definition of positive and negative angles of wave direction. The angles of wave attack at both dike arms β_N and β_P are calculated with Eq. (3) by considering the rotation of the dike (cf. Ch. 3.1). Unidirectional (long crested) and two types of multidirectional (short crested) waves were generated using a JONSWAP spectrum. Tab. 1 gives the tested angles of wave attack β_N and β_P and a summary of the test configuration.

$$\begin{aligned} &\text{for P - dike:} \quad \beta_P = \alpha - 15° \\ &\text{for N - dike:} \quad \beta_N = \alpha + 75 \end{aligned} \tag{3}$$

with: α wave direction with respect to the wave generator [°]
β_P angle of wave attack (P-dike) [°]
β_N angle of wave attack (N-dike) [°]

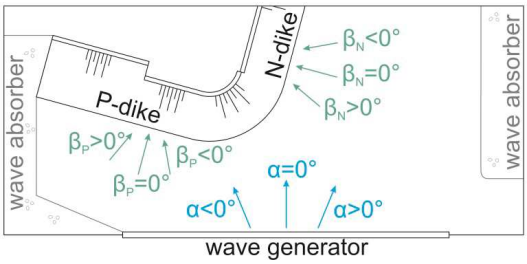

Figure 12: Definition of wave direction α and angle of wave attack β.

Table 1: Summary of test configuration.

crest height [m]	P-dike:	0.75						
	N-dike:	0.70						
freeboard height R_C [m]	P-dike:	0.15	0.10	0.07				
	N-dike:	0.10	0.05	0.02				
wave crestedness σ [°]	long crested waves: σ = 0° ("long ref")							
	short crested waves: σ = 34° ("short 1") and σ = 12° ("short 2")							
wave height H_S [m]	H_S	0.07	0.07	0.10	0.10	0.15	0.15	
and wave period T_p [s]	T_p	1.339	0.947	1.601	1.132	1.960	1.386	
angle of wave attack β [°]	P-dike:	-45	-30	-15	-7.5	0	+7.5	+15	+22.5
	N-dike:	+45	+60	+75	+82.5	+90	+97.5	+105	+112.5

4 Wave field analysis

4.1 Theory of wave fields

Information on the wave generation and wave parameters of tested wave fields is required for overtopping analyses. Furthermore, wave transformation processes may occur during wave overtopping model tests and have to be considered.

Theoretical wave spectra and directional distributions help defining the input (time-series of surface elevations) to generate wave fields for physical model tests. Sea states can be described with wave parameters, such as the significant wave height H_{m0} and average wave period $T_{m-1,0}$. These parameters are obtained from frequency domain or time domain analysis. Both types of analyses are described in MAI et al. (2004), MALCHEREK (2010) and HOLTHUIJSEN (2010).

The wave field evolution and wave overtopping behavior during model tests are affected to a great extent by wave transformation and wave breaking. A short description is given in the following.

Wave shoaling describes the phenomenon of changes in the wave height when waves approach perpendicularly from deep into shallow water. Approaching shallow water, the wave height and wave steepness increases due to shoaling until the orbital velocity exceeds the wave propagation velocity and the wave breaks. This process leads to a sudden decrease in wave height and energy dissipates.

Wave refraction describes the changes in wave direction when waves approach the shore obliquely, i. e. when the wave crests are not parallel to the depth contours. The rotation of the wave direction is a result of different water depths and consequently different propagation velocities along the oblique approaching wave crest. Besides the wave direction, the wave height is influenced. Refraction effects are expected during the CornerDike project when waves approach and run up the dike obliquely so that the wave direction rotates towards areas with shallower water (i. e. towards the dike structure).

Wave diffraction describes the propagation of waves behind obstructions (e. g. breakwaters or headlands) with zero water depth change. Passing an obstruction, the waves bend around this obstacle or waves spread out behind the opening due to wave energy transfer along wave rays. Diffraction descriptions are based on the Huygen's principle, which indicates that every point of a wave front is a source of a new wave that spreads out forward. Diffraction effects are expected during the CornerDike project at the wave field boundaries and near the dike during tests with $\beta > 90°$. These slightly

offshore waves move away from the dike and a shadow zone develops between the structure and the outer wave ray. According to Huygen's principle, new waves evolve in this area, which are then moving towards or along the dike.

Detailed information and mathematical descriptions on wave refraction and wave diffraction are given in MAI et al. (2004), HOLTHUIJSEN (2010), KAMPHUIS (2010) and MALCHEREK (2010).

4.2 General observations

Observations during the model tests and videos recorded during the experiments showed that the wave behavior and interaction with the structure depend on many factors, such as the wave direction, directional spread and further wave parameters. However, a general rough pattern of the wave behavior can be detected: Waves are redirected at the corner, then interact with approaching waves and finally slide along the N-dike in the form of wave rollers. A rough scheme of the observed wave behavior is shown in Fig. 13.

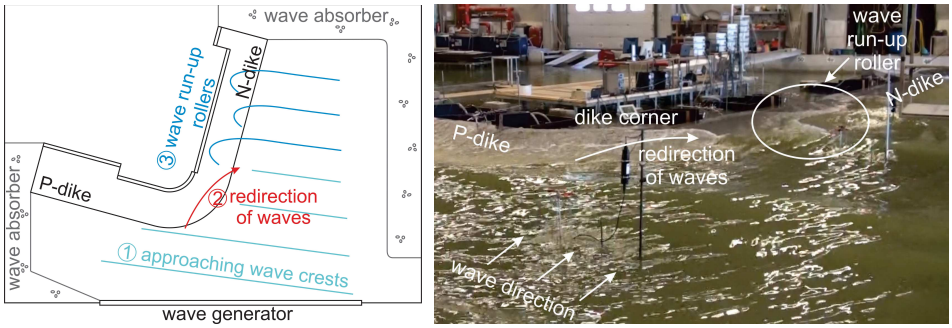

Figure 13: Rough scheme of wave development at the corner and N-dike (left) and wave pattern seen from wave generator (right) – long crested waves.

4.3 Comparison of measurement techniques

The wave field was measured at several positions with different measuring devices (see Ch. 3.2.1). Wave field signals obtained from records of the different measuring devices were processed with two types of analysis software (cf. Ch. 3.2.1) and the determined wave parameters were compared to each other. Slight differences were observed between the results of MIKE Zero and the WAFO-tool. A good agreement was found between the wave parameters obtained from the one-point-measurements (OPM) and wave arrays in a triangle-configuration (WA) calculated with the WAFO-tool. The model set-up included even a fifth wave array at the toe of the dike (WA7 in Fig. 6) while only four one-point-measurements were available. Therefore, further analyses are carried out with regard to the wave parameters obtained with WAFO from data of the triangle wave arrays.

4.4 Wave field development along the structure

The development of the wave height and wave period along the structure is of great interest for wave overtopping analyses. The evolution of the wave field, especially of the significant wave height and wave energy, is investigated on the one hand by analyzing model test data and on the other hand by performing numerical simulations.

4.4.1 Performing numerical simulations

To simulate the wave field evolution during CornerDike tests, a numerical wave model of the investigated dike structure was developed and simulations were performed with Delft3d-WAVE and the SWAN model. Three wave conditions are simulated numerically, which were tested during the laboratory investigations. The distribution of the significant wave height H_{m0} in the basin can be analyzed with the graphs given in Fig. 14.

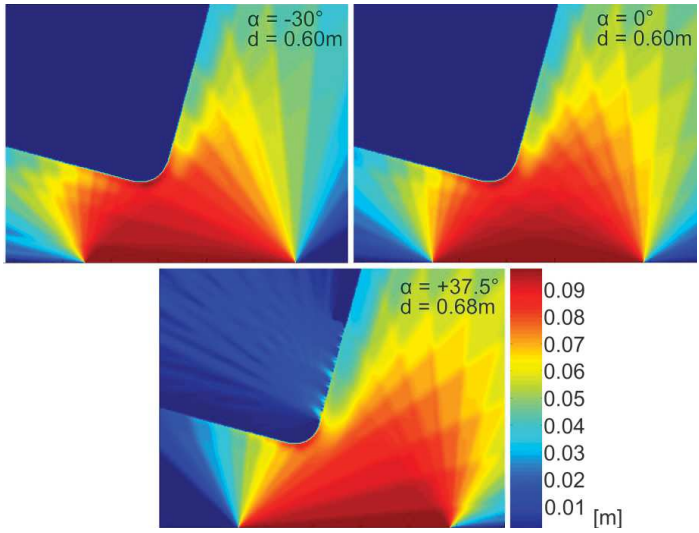

Figure 14: Wave height distribution – numerical results of test with α = -30° (top left), with α = 0° (top right) and with α = +37.5° (bottom).

Wave height concentrations (deep red areas) are detected right in front of the wave generator and at the dike corner. This means that the wave energy accumulates at the convex formed section of the dike and wave heights are increased in this area. Consequently, higher overtopping discharges are expected at the corner due to the wave energy maximum.

Furthermore, the significant wave height H_{m0} is investigated along a path (red line in sketch) and plotted against the distance from the starting point (see sketch) in Fig. 15. Fig. 15 shows that the wave height maximum is observed at the corner for all three simulations. Depending on the wave direction, it is relocated along the dike corner. Negative angles of wave attack (α = -30°) give a maximum wave height nearby the transition to the P-dike.

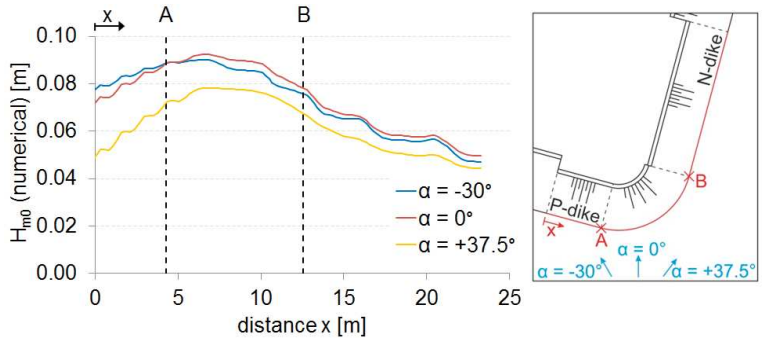

Figure 15: Evolution of significant wave height H_{m0} at toe of the structure along the dike line.

Increasing the angle of wave attack from α = -30° over α = 0° to α = +37.5° leads to a shift of the wave height maximum towards the middle of the corner. This means that also the position of the maximum wave energy depends on the wave direction. In general, the highest wave energy of each test exists at the dike corner. The wave energy decreases along the dike arms. Some small oscillations of the wave height can be detected at both dike arms, especially at the P-dike. These observations are ascribed to interactions between down-running and up-running waves.

4.4.2 Analyzing model test data

In the following, a reference position is chosen to compare the wave parameters at the investigated positions along the dike line. It is assumed that the wave parameters achieved from data of wave arrays in front of the wave generator are closest to the incident wave parameters. Therefore, WA1 is taken as a reference position. The ratio of the wave height H_{m0} (wave period $T_{m-1,0}$) of WAi (i = 3, …, 7) and wave height H_{m0} (wave period $T_{m-1,0}$) of WA1 are plotted against the measuring position (see Fig. 16 left). The same procedure is performed with the results of the numerical simulations (Fig. 16 right). Similar trends between the results of the laboratory tests and numerical simulations become apparent.

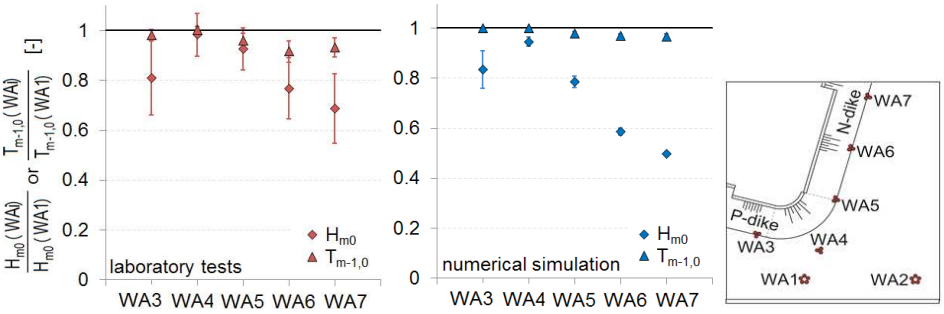

Figure 16: Development of wave height H_{m0} and wave period $T_{m-1,0}$ along the dike line from laboratory tests (left) and numerical simulation (right).

The wave period $T_{m-1,0}$ changes slightly along the dike line and the standard deviation is very small. In contrast, the wave height development shows a clear trend. Due to wave

diffraction and energy dissipation, the wave height decreases with increasing distance to the wave generator. WA4 (wave array in front of the corner) gives on average the same value as WA1. Moving along the N-dike, the wave height H_{m0} declines (cf. WA4 to WA7) down to a value of about 70 % of the wave height calculated at WA4.

4.4.3 Comparison of laboratory and numerical results

Wave parameters obtained from numerical simulations are now directly compared to the calculated wave parameters of the performed model tests. Therefore, the significant wave height H_{m0} and wave period $T_{m-1,0}$ determined numerically at the positions of the wave arrays are used. These values are plotted against the wave parameters calculated with data of the laboratory tests (see Fig. 17).

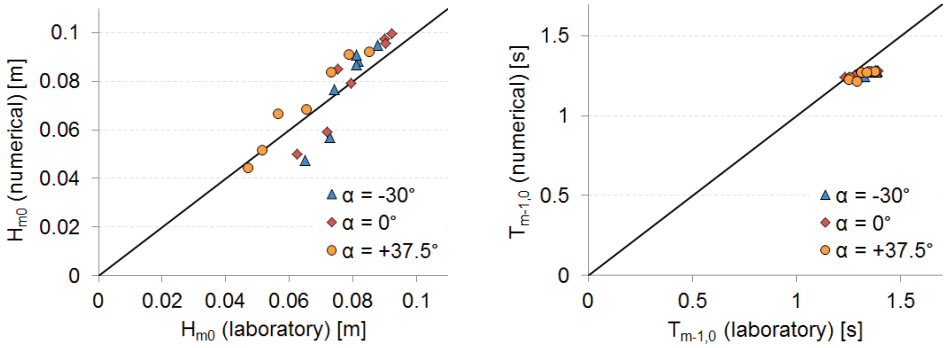

Figure 17: Comparison of wave parameters obtained from numerical simulations and laboratory tests – significant wave height H_{m0} left and mean wave period $T_{m-1,0}$ right.

In general, a good approximation between the results of the numerical simulations and model tests can be observed. The mean wave period $T_{m-1,0}$ is slightly underestimated by the numerical simulation for nearly all tests and measuring positions ($T_{num}/T_{lab} = 0.953 \pm 0.025$). The significant wave height H_{m0} is overestimated in most cases ($H_{num}/H_{lab} = 1.022 \pm 0.128$). Considering the fact that a calibration of the numerical model was omitted, results of the model test data correspond well to the results of the numerical simulation.

5 Wave overtopping analysis

5.1 Preliminary remarks

5.1.1 Terms and abbreviations

Several abbreviations and generalizations are used in the following sections. Tab. 2 gives an overview of the used abbreviations and their long forms. Since the used measuring devices are numbered (see Fig. 6), a control variable i is introduced to facilitate the differentiation between the instruments. Assigning a value to i leads to a clear definition of the addressed device, e. g. "OU3" stands for overtopping unit no. 3.

If no specific measuring device or several instruments are addressed, the general abbreviation is used and values for the control variable are defined in the context, e. g. "OUi with i = 1, 2" if overtopping units no. 1 and 2 are addressed.

Table 2: Explanation of used abbreviations.

abbreviation	long form / explanation
OUi	overtopping unit no. i with i = 1, …, 5
WAi	wave array no. i with i = 1, …, 7
OPMi	one-point-measurement no. i with i = 1, …, 4

5.1.2 Analysis restrictions

The reproduction of structures and natural processes is connected with simplifications and restrictions that have to be considered during analyses. One aspect of imperfect replications within the CornerDike project was the generated wave field as its width-development, which was limited due to the finite length of the wave generator (22 m). Consequently, some areas of the basin lay, depending on the direction of the generated wave field, outside the fully developed wave field. Signals of measuring instruments that were positioned in these areas have to be interpreted with caution or have to be neglected during analyses.

The evaluation whether measuring devices were influenced or not was carried out by considering the finite length of the wave generator, the wave direction and diffraction effects at the wave field boundaries. Data of measurement devices that were positioned outside the fully developed wave field and transition area is excluded from analyses.

5.2 Analysis of mean overtopping discharges

In a first step, the mean overtopping discharges q are analyzed without considering any measured wave parameters (cf. SCHERES et al. 2013). Wave overtopping rates of the investigated measuring positions are directly compared and the influence of the wave direction on wave overtopping is investigated. Within this first analysis, no mathematical descriptions or recommendations are given. It should rather provide a qualitative insight into wave overtopping behavior and influences on wave overtopping during the performed model tests.

Results show that the wave overtopping evolution along the dike line varies depending on the directional width. Short crested waves with a high directional spreading ($\sigma = 34°$) lead to decreasing wave overtopping discharges with increasing distance from the corner for all tested angles of wave attack. The development of mean overtopping discharges along the dike line of long crested and swell-like waves ($\sigma = 12°$) depends greatly on the wave direction.

Increased wave overtopping discharges were observed near the corner in the dike line for short crested waves with a directional spread $\sigma = 34°$ and small angles of wave attack ($|\beta| \leq 30°$). Increasing the angle of wave attack from $\beta = 45°$ upwards, in general decreasing overtopping discharges were observed during tests with multidirectional waves ($\sigma = 34°$).

5.3 Analysis of wave overtopping incorporating the wave parameters

Subsequently, the influence of the wave direction and corner in the dike line is analyzed incorporating the measured wave parameters at the toe of the dike. This analysis is undertaken with reference to the EURTOP-MANUAL (2007). Considering the wave parameters means that e. g. wave heights are taken into account by working with dimensionless parameters.

Empirical formulae describe the relationship between wave overtopping discharges and the freeboard height. Correction factors γ help to consider the influence of e. g. the roughness of the dike or oblique wave attack. Former investigations gave recommendations to consider the influence of oblique wave attack for angles of wave attack up to $\beta = 80°$. Yet, no validated guidance is given for $\beta > 80°$.

In the following, results of CornerDike tests with angles of wave attack up to 112.5° are analyzed and compared to previous investigations. Firstly, wave overtopping is analyzed separately for each tested wave crestedness. The influence of the directional spreading is analyzed at the end.

5.3.1 Approach of the analysis

Wave overtopping formulae are recommended in the EURTOP-MANUAL (2007) describing the relationship of the dimensionless overtopping discharge q^* and the relative freeboard height R_c^* (cf. Ch. 2). For analysis purposes the mentioned equations are rearranged into:

$$q^* = a \cdot \exp\left(-b \cdot R_c^*\right) \tag{4}$$

with: q^* dimensionless overtopping discharge [-]
R_c^* relative freeboard height [-]
a exponential regression coefficient (interception point with the y-axis) [-]
b exponential regression coefficient (slope of the regression curve) [-]

and

$$q^* = \frac{q}{\sqrt{g \cdot H_{m0}^3}} \cdot \frac{\sqrt{\tan\alpha}}{\xi_{m-1,0}} \qquad R_c^* = \frac{R_c}{\xi_{m-1,0} \cdot H_{m0}} \qquad a = 0.067 \quad \text{(br)} \tag{5}$$

respectively:

$$q^* = \frac{q}{\sqrt{g \cdot H_{m0}^3}} \qquad R_c^* = \frac{R_c}{H_{m0}} \qquad a = 0.2 \quad \text{(nbr)} \tag{6}$$

Wave parameters (H_{m0} and $T_{m-1,0}$) at the toe of the structure in front of each overtopping unit are substituted into the Eq. (4) to (6). In this case, the measured wave parameters, which are a combination of incident and reflected waves, are applied due to a missing reflection analysis.

An average coefficient b (see Eq. (4)) is calculated per overtopping unit OUi for tests with identical angles of wave attack and directional spreadings by performing an exponential regression analysis. The coefficient a in Eq. (4) is taken as a fixed interception point with the y-axis: 0.067 for breaking waves (br) and 0.2 for non-breaking waves (nbr)

(cf. EUROTOP-MANUAL 2007). Since the investigated dike was smooth with no berm or vertical wall on the slope, the correction factors γ_b, γ_f and γ_v are set to 1.0. In the following, the influence of oblique waves and a corner in the dike line is evaluated with the correction factor $\gamma_{\beta,c}$:

$$\gamma_{\beta,c} = \frac{b_{OUi,\beta}}{b_{ref}} \quad (i = 1, \ldots, 5) \tag{7}$$

with: $\gamma_{\beta,c}$ correction factor for oblique wave attack and a corner section in the dike line [-]
$b_{OUi,\beta}$ exponential coefficient for tests with β at OUi (i = 1, … , 5) [-]
b_{ref} exponential coefficient of the reference data (tests with β = 0° at OU2) [-]

5.3.2 Reference tests

Data of overtopping unit no. 2 (OU2) of tests with perpendicular waves (β_P = 0°) is used as reference data. Overtopping unit no. 1 (OU1) was positioned outside the fully developed wave field during tests with an angle of wave attack β_P = 0°. Results of the reference tests (β_P = 0° at OU2) of the three tested directional spreadings (σ = 0°, σ = 12° and σ = 34°) are presented in Fig. 18. The dimensionless overtopping rates q^* are plotted against the relative freeboard heights R_c^* (blue squares). Furthermore, the results of exponential regressions with a fixed intersection point with the y-axis according to Ch. 5.3.1 (blue, continuous line) are shown. Recommended formula for wave overtopping predictions of breaking waves (black, continuous line) of the EUROTOP-MANUAL (2007) and the 90 % confidence range (black, dotted lines) are illustrated in Fig. 18 as well.

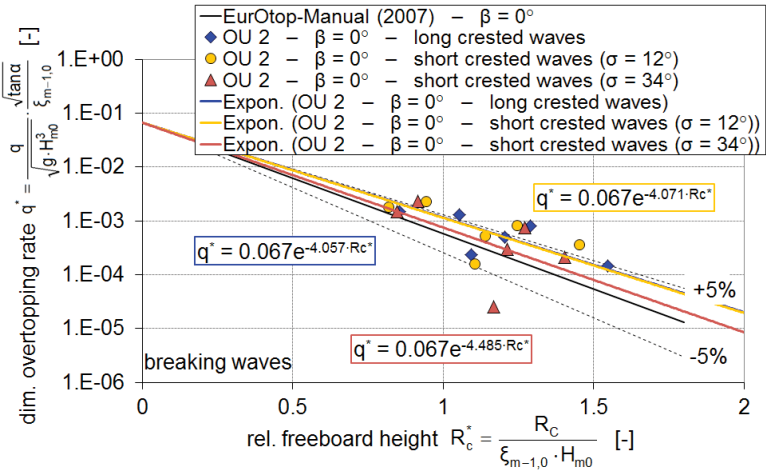

Figure 18: Dimensionless overtopping discharges of reference data: β_P = 0° at OU2.

Some data points are slightly higher than the predictions of the EUROTOP-MANUAL (2007), but most points fall within the 90 % confidence range. One point of short crested waves with σ = 34° lies beneath the predictions. A maximal difference of 15 % to the prediction formula (long crested waves) is found ($b_{ref,\sigma=0°}/b_{EurOtop}$ = -4.057/-4.75

= 85 %). The high differences are ascribed to the application of measured wave parameters instead of wave parameters of incident waves.

Overall, considering the lack of the incident wave parameters, the reference data corresponds quite well to the recommended formula of the EUROTOP-MANUAL (2007). For further analyses, the inclination of the slope b_{ref} of the reference data is compared to the slope inclinations b of further test conditions and overtopping units by determining correction factors $\gamma_{\beta,c}$.

5.3.3 Determination of correction factors

The b-coefficients of further CornerDike tests are calculated according to Ch. 5.3.1. Regression equations give the determined b-coefficients. For further analyses the correction factors $\gamma_{\beta,c}$ are determined with Eq. (7). By using the ratio of determined b-factors for further analyses, the influence of using the measured instead of incident wave parameters should be reduced to a great extent.

Non-breaking waves were observed during only about 5 % of all CornerDike tests. Consequently, the regression analyses for non-breaking waves are mostly based on a single point. Therefore, it is not reliable to include the data. In the following, only breaking waves are considered.

5.3.4 Influence of oblique wave attack – comparisons to former investigations

Wave overtopping at coastal structures under oblique wave attack with angles of wave attack β up to 80° was analyzed during previous experimental investigations. During the CornerDike project, angles of wave attack between -45° and +22.5° were tested at the P-dike and +45° to +112.5° at the N-dike (see Tab. 1). Previously determined correction factors $\gamma_{\beta,c}$ of CornerDike tests with $\beta \leq 75°$ and corresponding standard deviations are now plotted against the angle of wave attack β_P (for OU1 and OU2) and β_N (for OU3, OU4 and OU5) in Fig. 19 to Fig. 21. Results are presented separately for each investigated directional spreading. Different symbols help to distinguish between the correction factors of the probed overtopping units. A graphical legend in the top right of each figure illustrates which symbol corresponds to which overtopping unit. Fig. 12 shows the detailed definition of angles of wave attack. Recommendations of previous investigations (DE WAAL and VAN DER MEER 1992; OUMERACI et al. 2002; KORTENHAUS et al. 2006; EUROTOP-MANUAL 2007) are given in addition to the CornerDike results (black and grey lines). A similar wave overtopping behavior of swell-like waves ($\sigma = 12°$) and long crested waves is expected so that the recommended curves for long crested waves are used in the figure for short crested waves with $\sigma = 12°$ (cf. Fig. 20).

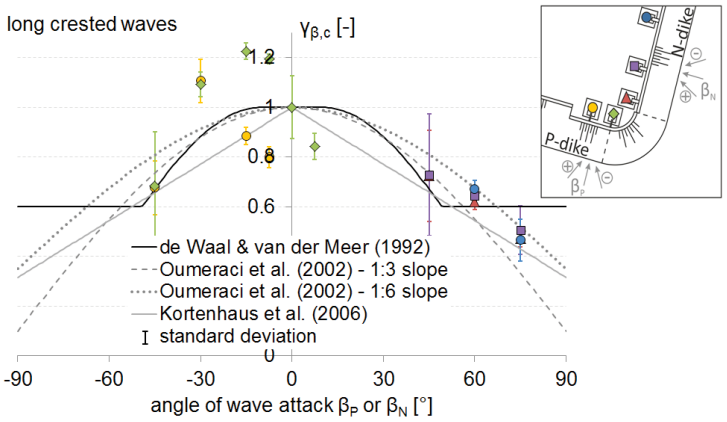

Figure 19: Correction factors $\gamma_{\beta,c}$ of CornerDike tests with angles of wave attack $\beta \leq 75°$ – long crested waves.

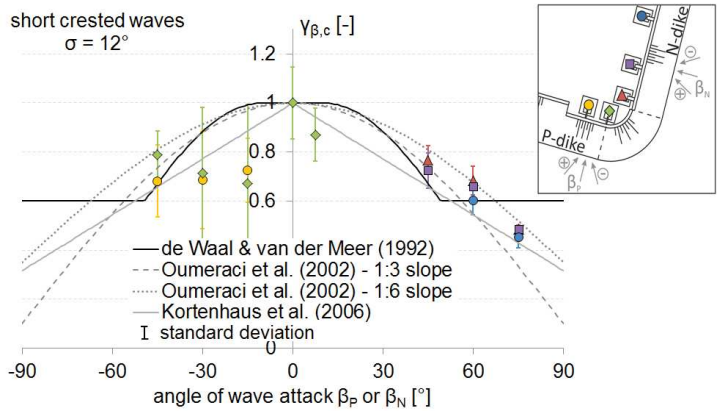

Figure 20: Correction factors $\gamma_{\beta,c}$ of Corner Dike tests with angles of wave attack $\beta \leq 75°$ – short crested waves ($\sigma = 12°$).

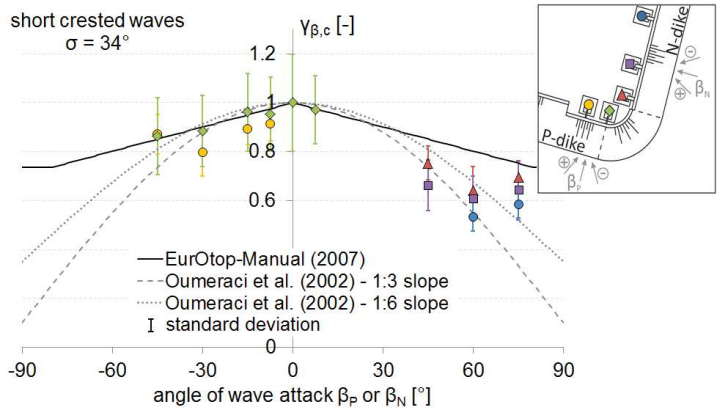

Figure 21: Correction factors $\gamma_{\beta,c}$ of CornerDike tests with angles of wave attack $\beta \leq 75°$ – short crested waves ($\sigma = 34°$).

The graphs show that the influence of oblique wave attack varies for the different directional widths and has to be examined separately for each wave crestedness. CornerDike results of tests with $\beta_P \leq 45°$ partly differ distinctively from recommended formulae (DE WAAL and VAN DER MEER 1992; EUROTOP-MANUAL 2007). Overall, correction factors $\gamma_{\beta,c}$ of $\beta_N \geq 45°$ fit well with the recommendations (e. g. OUMERACI et al. 2002). Differences between the correction factors of the overtopping units at the N-dike (OU3, OU4 and OU5) are very small. This means that the influence of the measuring position is largely considered in overtopping analyses: The wave parameters at the toe of the dike differ at the measuring positions as a result of wave transformation processes; due to incorporating the measured wave parameters in front of each overtopping unit into overtopping analyses, the influence of the wave field evolution is taken into account.

In front of the P-dike, only one wave array/one-point-measurement was installed. Wave parameters obtained from this device were used to calculate the dimensionless overtopping discharges and relative freeboard heights for OU1 as well as of OU2. Consequently, the evolution of wave parameters at the toe of the dike is not taken into account for these overtopping units. This leads to some significant differences between the correction factors of OU1 and OU2 (green and yellow symbols in Fig. 19 to Fig. 21). For long crested and swell-like waves ($\sigma = 12°$), the correction factor is for $\beta_P = 7.5°$ much lower than for perpendicular wave attack ($\beta_P = 0°$). This observation can be ascribed to diffraction effects at the wave field boundaries that affect the wave parameters and wave overtopping (cf. Ch. 5.1.2). For $|\beta_P| \leq 45°$, the results of long crested and short crested waves with $\sigma = 12°$ were assumed to be almost equal. However, converse results were obtained: The correction factors of long crested waves increase at first (maximum correction factor for $|\beta_P| = 15°$ at OU2 and $|\beta_P| = 30°$ at OU1, cf. Fig. 19), then they decrease again; the opposite can be observed for swell-like waves ($\sigma = 12°$, cf. Fig. 20).

Overall, the reliability of CornerDike tests is proven. Correction factors for angles of wave attack $\beta \geq 45°$ match well with the recommendations and the model tests are assessed as reliable.

5.3.5 Influence of a corner in the dike line for $\beta \leq 45°$

Differences for $\beta \leq 45°$ between CornerDike results and the recommendations (DE WAAL and VAN DER MEER 1992; EUROTOP-MANUAL 2007) are ascribed to effects of the dike corner. Results of tests with $\beta \leq 45°$ at the P-dike are analyzed in-depth subsequently.

The correction factors of short crested waves with $\sigma = 34°$ and $|\beta_P| \leq 45°$ correspond well to the results of former investigations. Still, the standard deviation is high for these tests (see Ch. 5.3.4). Furthermore, long crested and short crested waves with $\sigma = 12°$ show for $|\beta_P| \leq 45°$ unexpectedly converse results and high standard deviations (see Ch. 5.3.4). Plotting the correction factors against the angle of wave attack for each test separately, it becomes obvious that the correction factors $\gamma_{\beta,c}$ do not only depend on the angle of wave attack β_P but also on the significant wave height H_s and wave steepness s_{0p}. Increasing correction factors can be observed for increasing wave heights. Furthermore, shallow waves ($s_{0p} = 0.025$) lead to higher correction factors than steeper

waves (s_{0p} = 0.050). Depending on the deep water wave height H_s and wave steepness s_{0p}, the obtained correction factors $\gamma_{\beta,c}$ are higher or smaller than the recommendations (DE WAAL and VAN DER MEER 1992; EUROTOP-MANUAL 2007) given for γ_β. Therefore, two groups of waves are differentiated in order to analyze the results presented above:

- waves that lead to correction factors $\gamma_{\beta,c}$ above recommendations (WC1, WC2 & WC3)
- waves that lead to correction factors $\gamma_{\beta,c}$ below recommendations (WC4, WC5 & WC6 for long crested and short crested waves with σ = 12° or WC4 & WC6 for short crested waves with σ = 34°)

Investigating the influence of the corner in the dike line, the curve of DE WAAL and VAN DER MEER (1992) is taken as a reference for long crested and swell-like waves (σ = 12°) and the recommendations of the EUROTOP-MANUAL (2007) for short crested waves (σ = 34°). The correction factors for a corner in the dike line γ_c are determined as the ratio between the correction factors $\gamma_{\beta,c}$ and recommended correction factors γ_β (see Eq. (8)).

$$\gamma_c = \frac{\gamma_{\beta,c}(\text{of CornerDike tests})}{\gamma_\beta(\text{of EurOtop - Manual 2007 or de Waal \& van der Meer 1992})} \tag{8}$$

with: γ_c correction factor for a corner in the dike line [-]
$\gamma_{\beta,c}$ correction factor for oblique wave attack and a corner in the dike line [-]
γ_β correction factor for oblique wave attack [-]

Subsequently, the calculated correction factors γ_c are plotted against the angle of wave attack β_P in Fig. 22 to Fig. 24. Each wave condition (WC) is defined by a colored symbol and line. Regression analyses are performed separately for both groups of waves.

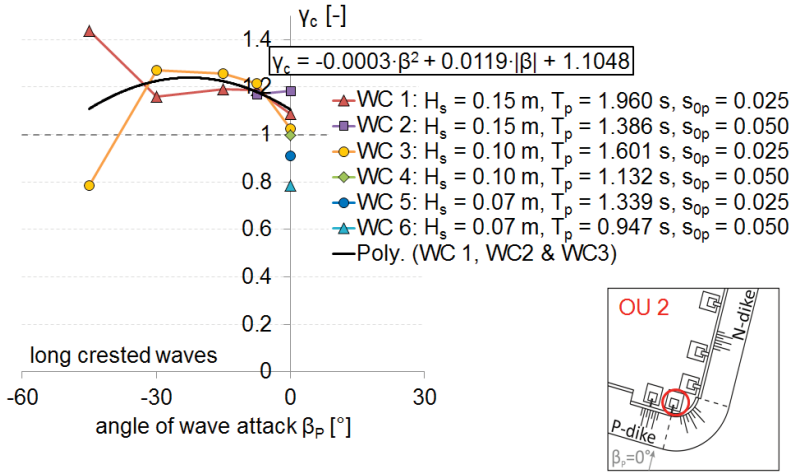

Figure 22: Correction factors γ_c of CornerDike tests at OU2 for each test separately – long crested waves.

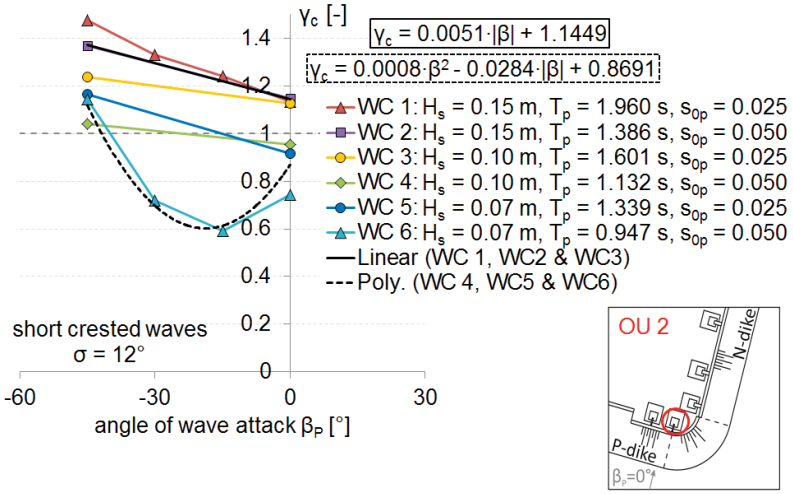

Figure 23: Correction factors γ_c of CornerDike tests at OU2 for each test separately – short crested waves ($\sigma = 12°$).

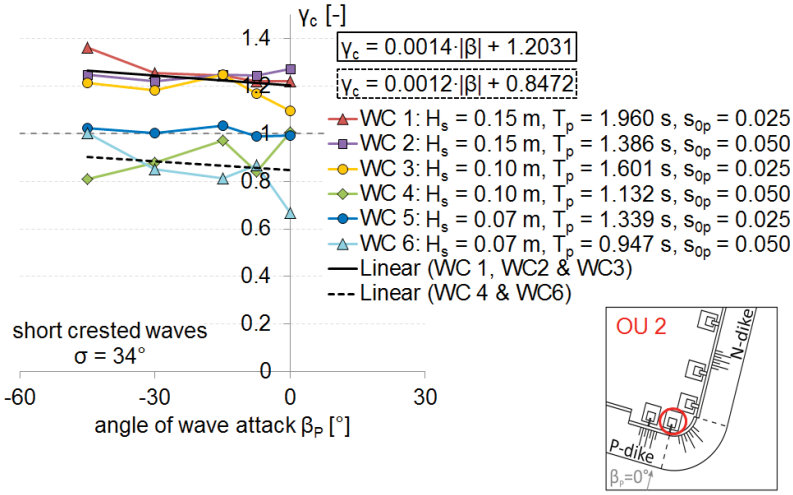

Figure 24: Correction factors γ_c of CornerDike at OU2 for each test separately – short crested waves ($\sigma = 34°$).

A summary of the obtained formulae to consider the influence of a corner in the dike line for $\beta \leq 45°$ is given in Ch. 6. No recommendations can be given how to incorporate the influence of a corner in the dike line for $\beta \leq 45°$ at parts of the dike with a distance from the corner $\geq 3 \cdot h_{dike}$ as no tests were performed with $\beta_N \leq 45°$.

As a last step, the evidence of the obtained equations is proven by revising the correction factors $\gamma_{\beta,c}$ of CornerDike tests with $\beta \leq 45°$ using Eq. (9). This means that the influence of the corner in the dike line is deducted and γ_β is calculated. The obtained correction factors γ_β are compared to recommendations of former investigations (see Fig. 25). Deducting the influence of the corner, the correction factors of CornerDike tests match well to existing test results.

$$\gamma_\beta(\text{of CornerDike tests}) = \frac{\gamma_{\beta,c}(\text{of CornerDike tests})}{\gamma_c(\text{with (6.12) to (6.17)})} \tag{9}$$

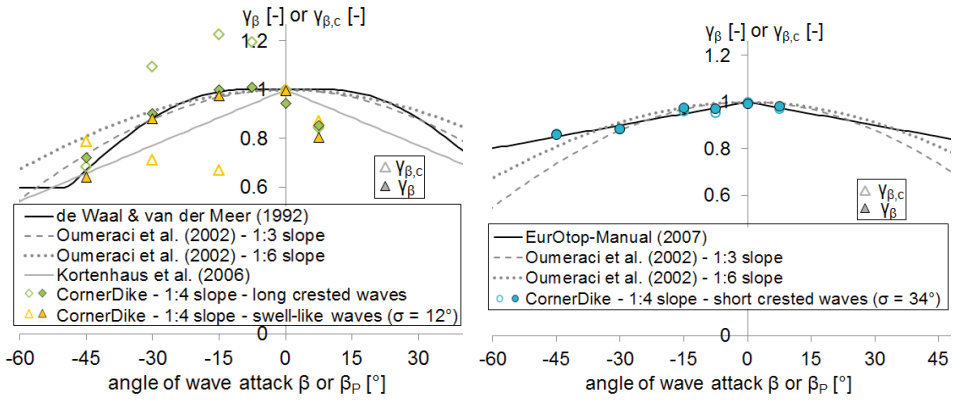

Figure 25: Correction factors $\gamma_{\beta,c}$ of CornerDike tests with $\beta \leq 45°$ compared to former investigations.

5.3.6 Influence of very oblique waves ($45° \leq \beta \leq 90°$) and slightly offshore waves ($\beta > 90°$)

No validated guidance for wave overtopping predictions is given for very oblique and slightly offshore waves ($\beta > 80°$). Angles of wave attack between +45° to +112.5° were tested at the N-dike during the CornerDike project (see Tab. 1). These tests are analyzed in the following. Plotting the calculated correction factors $\gamma_{\beta,c}$ and corresponding standard deviations of these tests against the angle of wave attack β_N for OU3, OU4 and OU5 (positioned behind the N-dike), the different wave overtopping behavior of long crested and short crested waves becomes obvious. In the following, the results of long crested waves are evaluated in combination with the results of swell-like waves ($\sigma = 12°$) as similar wave overtopping behavior is expected. Afterwards, short crested waves with $\sigma = 34°$ are analyzed separately.

For long crested and swell-like ($\sigma = 12°$) waves, equal correction factors exist for $\beta_N \leq 75°$ at the transition from the corner to the dike arm (OU3) and along the N-dike (OU4 & OU5). This means that no influence of the corner is detected for angles of wave attack between 45° and 75°. The difference between long crested and swell-like waves is very small for these wave directions. For $\beta_N \geq 82.5°$, higher correction factors $\gamma_{\beta,c}$ are given for OU4 and OU5 compared to OU3. It is assumed, that influences of the corner lead to continuously decreasing $\gamma_{\beta,c}$ of OU3 while the correction factors of OU4 and OU5 increase for parallel and slightly offshore waves compared to waves with $\beta_N = 75°$. The increase of $\gamma_{\beta,c}$ of OU4 and OU5 is ascribed to diffraction and refraction effects. Hence, recommendations are given on the one hand at the transition from the corner to the dike arm (OU3) and on the other hand for parts of the straight-aligned dike arm with a distance from the corner $\geq 3 \cdot h_{dike}$ (OU4 and OU5).

Regression analyses were conducted using Microsoft Excel and SPSS Statistics. Objective of these analyses is the development of formulae that describe the relationship

between correction factors $\gamma_{\beta,c}$ and angles of wave attack β. Fig. 26 to Fig. 29 show the results for long crested and swell-like waves (σ = 12°). Correction factors of CornerDike tests, corresponding trend lines and recommendations of former investigations (DE WAAL and VAN DER MEER 1992; OUMERACI et al. 2002; KORTENHAUS et al. 2006; EUROTOP-MANUAL 2007) are given. To obtain formulae that represent the whole range of wave directions (0° to 105°/112.5°), auxiliary values (black diamonds) were incorporated into these regression analyses. For long crested and swell-like waves (σ = 12°), these auxiliary values were determined with design guidance given by DE WAAL and VAN DER MEER (1992), whose reliability was proven in previous investigations (cf. VAN DER MEER 2010).

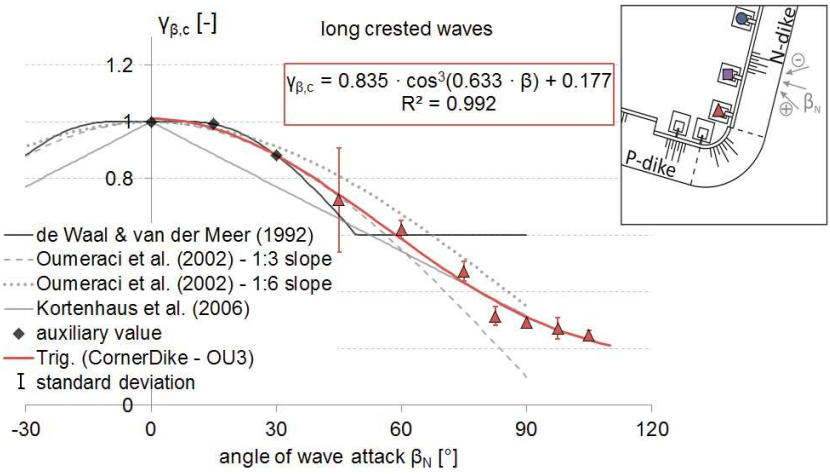

Figure 26: Regression analysis for the transition from the corner to the N-dike (OU3) – long crested waves.

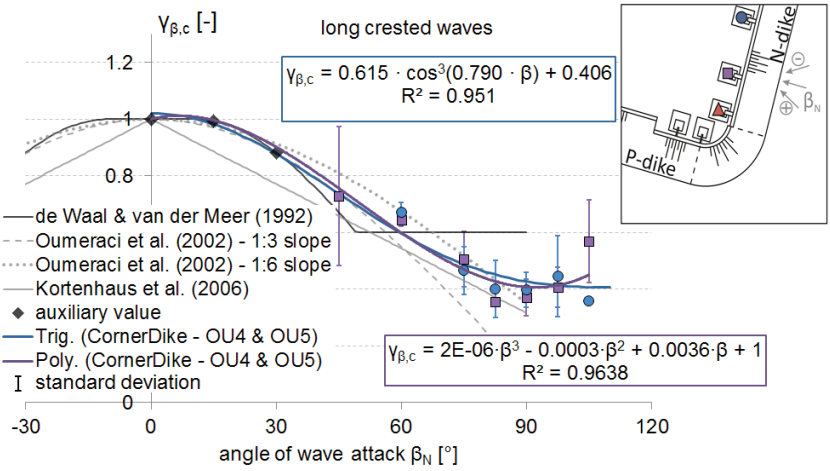

Figure 27: Regression analysis for the straight-aligned dike arm (OU4 & OU5) – long crested waves.

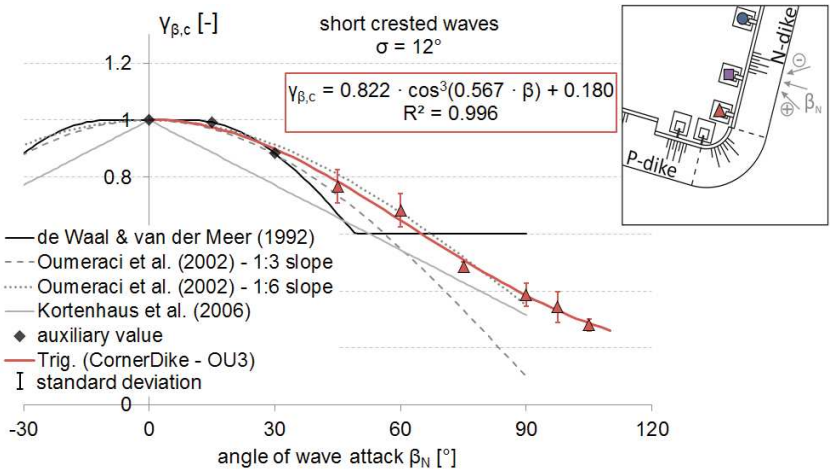

Figure 28: Regression analysis for the transition from the corner to the N-dike (OU3) – short crested waves (σ = 12°).

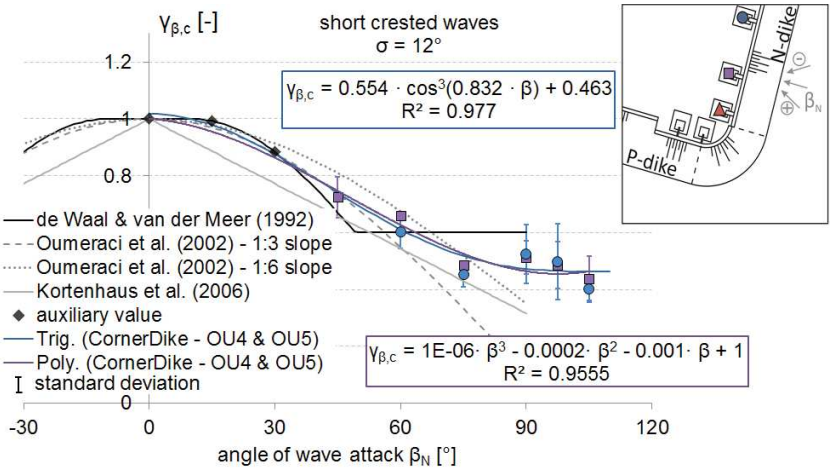

Figure 29: Regression analysis for the straight-aligned dike arm (OU4 & OU5) – short crested waves (σ = 12°).

Determined trend lines approximate the correction factors very well and are for small angles of wave attack (β < 45°) quite similar to recommendations given by DE WAAL and VAN DER MEER (1992). Looking at Fig. 27 (regression analysis for the straight-aligned dike arm (OU4 & OU5) for long crested waves) it is noticeable that the polynomial trend line leads to a more precise approximation. However, the trigonometric function is seen as more reasonable.

The influence of very oblique and slightly offshore, long crested and swell-like (σ = 12°) has been analyzed. Subsequently, short crested waves with σ = 34° and β ≥ 45° are investigated.

The results of short crested waves with σ = 34° yield, compared to long crested and swell-like waves, an irregular pattern (see Fig. 30). Correction factors $\gamma_{\beta,c}$ show several

minima and maxima with increasing angles of wave attack. In general, slight differences between the $\gamma_{\beta,c}$ of the three overtopping units exist. For $\beta_N \leq 75°$, OU3 shows the highest correction factors; this changes for $\beta_N \geq 82.5°$. Correction factors of OU4 are for all wave directions slightly higher than the ones of OU5. A significant difference between the correction factor for $\beta_N = 45°$ at the N-dike and the correction factor for $|\beta_P| = 45°$ at the P-dike (see Fig. 22) was noticed. This deviation is ascribed to the width-limit of the wave generator and diffraction effects at the wave field boundaries: Every wave of a multidirectional wave field has a different wave direction as a result of the directional spread; the less oblique approaching waves (single waves with $\beta_N \leq 15°$ e. g. during tests with $\beta_N = 45°$ and $\sigma = 34°$) do not reach the N-dike due to the finite length of the wave generator and consequently the test results are influenced by model effects. Therefore, correction factors for $|\beta| = 45°$ are lower at the N-dike than at the P-dike (see Fig. 22). This restriction is also present for $\beta_N = 60°$. Hence, the correction factors for $\beta_N = 45°$ and $\beta_N = 60°$ of short crested waves with $\sigma = 34°$ are excluded from subsequent regression analyses.

Results of the regression analysis for short crested waves with $\sigma = 34°$ are illustrated in Fig. 30. Regressions were performed for the transition from the corner to the dike arm (OU3, red curve) and for the straight-aligned dike (OU4 & OU5, violet curve). Auxiliary values (black diamonds) were calculated using the recommendations of the EUROTOP-MANUAL (2007). Correction factors of the CornerDike project that were excluded from regression analyses (see paragraph above) are illustrated with transparent symbols ($\beta = 45°$ and $\beta = 60°$).

The deviations from determined trend lines are slightly higher than during the analysis of long crested and swell-like waves. However, the trends of the correction factors are described with the given formulae. Additionally, an intersection point at $\beta \approx 90°$ between both regression lines is obtained so that the wave overtopping behavior along the dike line is reproduced ($\beta < 90°$ higher correction factors at OU3, $\beta \geq 90°$ lower correction factors at OU3 than at OU4 & OU5). A summary of obtained formulae to consider the influence of a corner in the dike line for $\beta \geq 45°$ is given in Ch. 6.

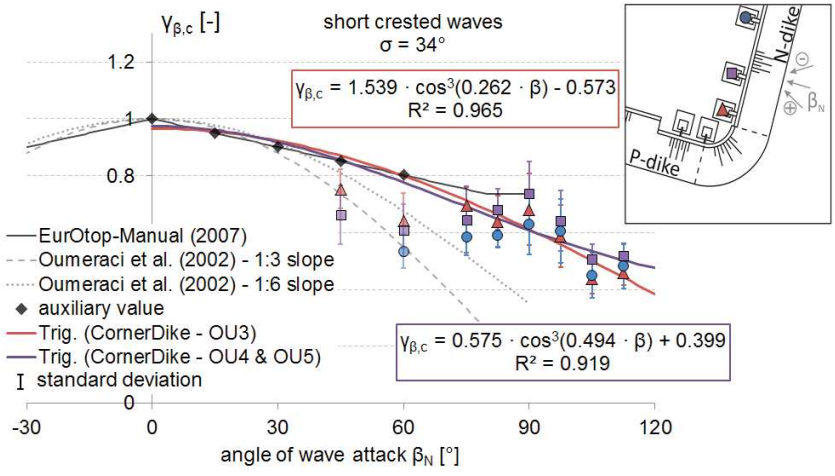

Figure 30: Regression analysis for the transition from the corner to the N-dike (OU3) and straight-aligned dike arm (OU4 & OU5) – short crested waves ($\sigma = 34°$).

5.3.7 Influence of the directional spreading

The CornerDike reference data has shown differences between the tested directional spreadings. Therefore, the wave overtopping analyses were conducted separately for each wave crestedness. The influence of the directional spreading on wave overtopping is herein investigated by comparing the reference b-factors of long crested waves and short crested waves. For this analysis, the correction factors γ_σ of the reference data are redetermined with Eq. (10).

$$\gamma_\sigma = \frac{b_{OU2,\beta=0°,\sigma}}{b_{OU2,\beta=0°,\sigma=0°}} \tag{10}$$

with: γ_σ correction factor for directional spreading [-]
$b_{OU2,\beta=0°,\sigma}$ exponential coefficient for tests with $\beta = 0°$ and σ at OU2 [-]
$b_{OU2,\beta=0°,\sigma=0°}$ exponential coefficient for tests with $\beta = 0°$ and $\sigma = 0°$ at OU2 [-]

The redetermined correction factors γ_σ are plotted against the corresponding directional spreading in Fig. 31. Furthermore, the correction factors and recommendations by KORTENHAUS et al. (2006) for breaking waves are shown.

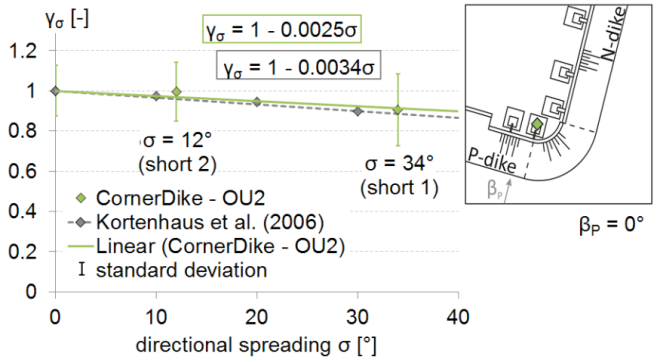

Figure 31: Correction factors γ_c of CornerDike tests with $\beta = 0°$ at OU2.

The influence of the directional width can be described with Eq. (11):

$$\gamma_\sigma = 1 - 0.0025 \cdot \sigma \tag{11}$$

with: γ_σ correction factor for directional spreading [-]
σ directional width [°]

The deviation between CornerDike results and KORTENHAUS et al. (2006) is very small and the results are confirmed due to the good fit.

6 Summary and conclusions

The main objective of this study was to extend the knowledge on wave overtopping processes and the influence of very oblique waves and a corner in the dike line on wave overtopping. Therefore, model tests were conducted in the CornerDike project on a 1:4 sloped, convex dike in the shallow water basin of DHI in Hørsholm, Denmark. Wave

run-up and wave overtopping was investigated during tests with long crested and short crested waves with angles of wave attack between -45° to +112.5°.

Relevant equations that describe the relationship between mean wave overtopping discharges and the freeboard height are given in the EUROTOP-MANUAL (2007). Correction factors γ help to consider the influence of e. g. the roughness of the dike surface or oblique wave attack.

The correction factors γ of CornerDike tests have been determined and analyzed. Formulae for the correction factors γ_β (influence of oblique wave attack), γ_c (influence of a corner in the dike line) and γ_σ (influence of the directional width) have been developed and are recommended for future wave overtopping predictions or comparisons with further investigations.

Results showed that the influence of a corner in the dike line γ_c depends for $\beta \leq 45°$ on the angle of wave attack β as well as on the deep water wave height H_s and wave steepness s_{0p}. Correction factors $\gamma_{\beta,c}$ have been developed from test data of waves with $45° \leq \beta \leq 112.5°$ (very oblique and slightly offshore waves). Formulae for γ_β are given at the transition from the corner to the straight-aligned dike arm and for positions on the dike arm with a distance from the corner $\geq 3 \cdot h_{dike}$ for each directional spreading separately.

Table 3: Recommended formulae for γ_β and $\gamma_{\beta,c}$ at the transition from corner to dike arm (distance to corner < $3 \cdot h_{dike}$).

transition corner to dike arm	long crested waves	$\lvert\beta\rvert < 10°$:	$\gamma_\beta = 1.0$
		$10 \leq \lvert\beta\rvert < 30°$:	$\gamma_\beta = \cos^2(\lvert\beta\rvert - 10°)$
		$\lvert\beta\rvert \geq 30°$:	γ_β or $\gamma_{\beta,c} = 0.835 \cdot \cos^3(0.633 \cdot \lvert\beta\rvert) + 0.177$
	swell-like waves (σ = 12°)	$\lvert\beta\rvert < 10°$:	$\gamma_\beta = 1.0$
		$10 \leq \lvert\beta\rvert < 25°$:	$\gamma_\beta = \cos^2(\lvert\beta\rvert - 10°)$
		$\lvert\beta\rvert \geq 25°$:	γ_β or $\gamma_{\beta,c} = 0.822 \cdot \cos^3(0.567 \cdot \lvert\beta\rvert) + 0.180$
	short crested waves (σ = 34°)	$\lvert\beta\rvert < 60°$:	γ_β or $\gamma_{\beta,c} = 1 - 0.0033 \cdot \lvert\beta\rvert$
		$\lvert\beta\rvert \geq 60°$:	$\gamma_{\beta,c} = 1.539 \cdot \cos^3(0.262 \cdot \lvert\beta\rvert) + 0.573$

Table 4: Recommended formulae for γ_β and $\gamma_{\beta,c}$ for parts of the dike with a distance $\geq 3 \cdot h_{dike}$ from the corner.

distance ≥ 3·hdike from corner	long crested waves	$\lvert\beta\rvert < 10°$:	$\gamma_\beta = 1.0$
		$10 \leq \lvert\beta\rvert < 30°$:	$\gamma_\beta = \cos^2(\lvert\beta\rvert - 10°)$
		$\lvert\beta\rvert \geq 30°$:	γ_β or $\gamma_{\beta,c} = 0.615 \cdot \cos^3(0.790 \cdot \lvert\beta\rvert) + 0.406$
	swell-like waves (σ = 12°)	$\lvert\beta\rvert < 10°$:	$\gamma_\beta = 1.0$
		$10 \leq \lvert\beta\rvert < 30°$:	$\gamma_\beta = \cos^2(\lvert\beta\rvert - 10°)$
		$\lvert\beta\rvert \geq 30°$:	γ_β or $\gamma_{\beta,c} = 0.554 \cdot \cos^3(0.832 \cdot \lvert\beta\rvert) + 0.463$
	short crested waves (σ = 34°)	$\lvert\beta\rvert < 45°$:	$\gamma_\beta = 1 - 0.0033 \cdot \lvert\beta\rvert$
		$\lvert\beta\rvert \geq 45°$:	$\gamma_{\beta,c} = 0.575 \cdot \cos^3(0.494 \cdot \lvert\beta\rvert) + 0.399$

Recommendations for γ_β and $\gamma_{\beta,c}$ for waves that first have to pass the corner before or while running up the dike (i. e. positive β, cf. legend in Fig. 32 are given in Tab. 3 and Tab. 4 (γ_β given for $\beta \leq 45°$ and $\gamma_{\beta,c}$ for $\beta > 45°$). Fig. 32 illustrates the given equations. Furthermore, it is recommended to use the formulae given in Tab. 5 for γ_c to consider the influence of a corner in the dike line at the transition from the corner to the dike arm for angles of wave attack $0 \leq \beta \leq 45°$.

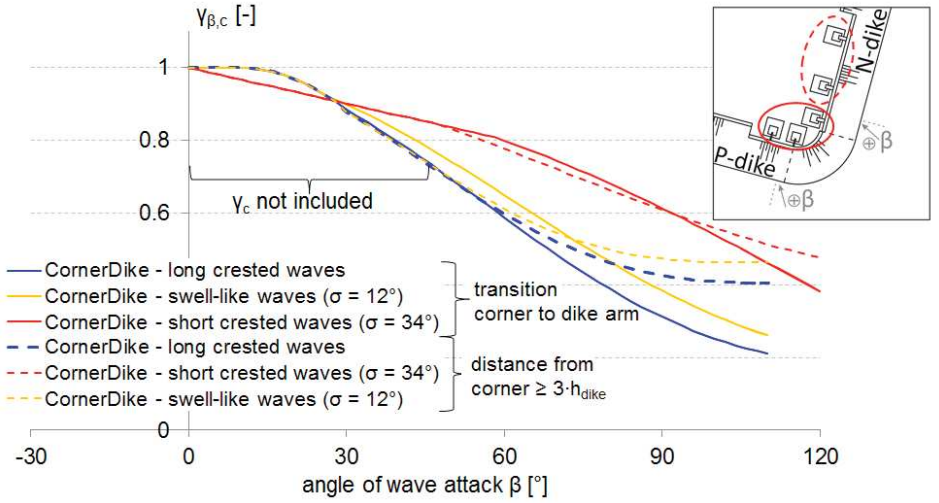

Figure 32: Recommendations of Tab. 3 and Tab. 4 to consider the influence of very oblique wave attack and a corner in the dike line.

Table 5: Recommended formulae for γ_c at the transition from the corner to the dike arm (distance to corner < $3 \cdot h_{dike}$) for $\beta \leq 45°$.

	$H_s/h_{dike} = 0.2$, all steepnesses or $H_s/h_{dike} = 0.133$, shallow waves ($s_{0p} = 0.025$)	$H_s/h_{dike} = 0.133$, steep waves ($s_{0p} = 0.050$) or $H_s/h_{dike} = 0.1$, all steepnesses [for σ = 34°: without $H_s/h_{dike} = 0.1$, $s_{0p} = 0.050$]
long crested waves	$\gamma_c = -0.0003 \cdot \beta^2 + 0.0119 \cdot \lvert\beta\rvert + 1.1048$	no recommendations possible
swell-like waves (σ = 12°)	$\gamma_c = 0.0051 \cdot \lvert\beta\rvert + 1.1449$	$\gamma_c = 0.0008 \cdot \beta^2 - 0.0284 \cdot \lvert\beta\rvert + 0.8691$
short crested waves (σ = 34°)	$\gamma_c = 0.0014 \cdot \lvert\beta\rvert + 1.2031$	$\gamma_c = 0.0012 \cdot \lvert\beta\rvert + 0.8472$

Lastly, the influence of the wave crestedness on wave overtopping was analyzed. The influence of the directional width can be described with Eq. (12).

$$\gamma_\sigma = 1 - 0.0025 \cdot \sigma \tag{12}$$

First analyses on wave overtopping and wave run-up (see WOLF 2013) are successfully undertaken within the CornerDike project. Analyzing data of the CornerDike model tests can still be continued, e. g. analyses concerning the flow processes on the dike crest or a detailed analysis of the wave field are desirable.

7 Acknowledgement

This work was supported by the European Community's Seventh Framework Programme through the grant to the budget of the Integrating Activity HYDRALAB IV, contract no. 261520. The authors thank the EU for funding the CornerDike project and the project partners for the great cooperation. The contribution of the Danish Hydraulic Institute (DHI) in Hørsholm (Denmark) by providing access to the hydraulic laboratory and scientific support during the physical model tests is also highly acknowledged.

Furthermore, the authors wish to express their thanks to the German Ministry of Education and Research (BMBF) for the support of the follow-up project ConDyke within a KFKI-project, project-no. 03KIS0108 (RWTH Aachen University) and 03KIS0109 (Leibniz Universität Hannover).

8 References

DE WAAL, J. P. and VAN DER MEER, J. W.: Wave run-up and overtopping on coastal structures. In: Proceedings of the 23th International Conference on Coastal Engineering. Venice, Italy, 23, 1758–1771, 1992.

EURTOP-MANUAL: Pullen, T.; Allsop, N. W. H.; Bruce, T.; Kortenhaus, A.; Schüttrumpf, H. and van der Meer, J. W.: EurOtop - Wave overtopping of sea defences and related structures: Assessment manual. Die Küste, 73, 2007.

FRANCO, C.; FRANCO, L.; RESTANO, C. and VAN DER MEER, J. W.: The effect of wave obliquity and short crestedness on the overtopping rate and volume distribution on caisson breakwaters. Final Project Proceedings, MAST II, MCS-Project: Monolithic Coastal Structures. 37 pp., 1995.

HOLTHUIJSEN, L. H.: Waves in oceanic and coastal waters. Cambridge University Press, 404 pp., 2010.

KAMPHUIS, J. W.: Introduction to Coastal Engineering and Management. In: Advanced Series on Ocean Engineering, 30. World Scientific Publishing Company, Incorporated. 564 pp., 2010.

KORTENHAUS, A.; GEERAERTS, J. and HASSAN, R.: Wave run-up and overtopping of sea dikes with and without stilling wave basin under 3D wave attack. DIKE-3D. Final Report. Braunschweig, Germany, 2006.

LORKE, ST.; BRÜNING, A.; VAN DER MEER, J. W.; SCHÜTTRUMPF, H.; BORNSCHEIN, A.; GILLI, ST.; POHL, R.; SCHLÜTTER, F.; SPANO, M.; RIHA, J. and WERK, ST.: On the effect of current on wave run-up and wave overtopping. In: Proceedings of the 32nd International Conference on Coastal Engineering. Shanghai, China, 2010.

MAI, S.; PAESLER, CH. und ZIMMERMANN, C.: Wellen und Seegang an Küsten und Küstenbauwerken. Vorlesungsergänzungen des Lehrstuhls für Wasserbau und Küsteningenieurwesen, Franzius-Institut, Universität Hannover, Germany, 2004.

MALCHEREK, A.: Gezeiten und Wellen. Die Hydromechanik der Küstengewässer. Vieweg+Teubner Verlag, Wiesbaden, 301 pp., 2010.

NAPP, N.; BRUCE, T.; PEARSON, J. and ALLSOP, W.: Violent overtopping of vertical seawalls under oblique wave conditions. In: Proceedings of the 29th International Conference of Coastal Engineering. Lisbon, Portugal, 4482–4493, 2004.

NAPP, N.; PEARSON, J.; RICHARDSON, ST.; BRUCE, T.; ALLSOP, W. and PULLEN, T.: Overtopping of seawalls under oblique and 3-D wave conditions, In: Proceedings of the 28th International Conference on Coastal Engineering. Cardiff, United Kingdom, 2178–2190, 2002.

OPENSTREETMAP: Die freie Wiki-Weltkarte.
Accessed 7 April 2013: http://www.openstreetmap.org/
License: http://www.openstreetmap.org/copyright/en.

OUMERACI, H.; MÖLLER, J.; SCHÜTTRUMPF, H.; ZIMMERMANN, C.; DAEMRICH, K.-F. und OHLE, N.: Schräger Wellenauflauf an Seedeichen. Abschlussbericht zum BMBF Forschungsprojekt KIS 015/016. LWI Report No. 881 / FI Report No. 643/V. Braunschweig, Germany, 2002.

OUMERACI, H.; MÖLLER, J.; SCHÜTTRUMPF, H.; ZIMMERMANN, C.; DAEMRICH, K.-F. and OHLE, N.: Influence of oblique wave attack on wave run-up and wave overtopping – 3D model tests at NRC/Canada with long and shorts crested waves. LWI Report No. 859 / FI Report No. 643. Braunschweig, Germany, 2001.

SAKAKIYAMA, T. and KAJIMA, R.: Wave overtopping and stability of armor units under multidirectional waves. In: Proceedings of 25th Conference on Coastal Engineering. Orlando, Florida, 1862–1875, 1996.

SCHERES, B.; LORKE, ST.; POHL, R.; VAN DER MEER, J. W. and SCHÜTTRUMPF, H.: The effect of very oblique waves on wave overtopping at a convex formed sea dike. In: Proceedings of the 6th International Short Course/Conference on Applied Coastal Research (6th SCACR). Lisbon, Portugal, 2013.

VAN DER MEER, J. W.: Influence of wind and current on wave run-up and wave overtopping. Detailed analysis on the influence of current on wave overtopping. Hydralab – Flowdike report, 2010.

WOLF, V.: Schräger und gerader Wellenauflauf an speziellen Deichformen. Dresden, Germany, unpublished diploma thesis, 2013.